

# Phase locking in a two-element laser array: a test of the coupled-oscillator model

Jingwen Xu, Shiqun Li, K. K. Lee, and Y. C. Chen

Department of Physics and Astronomy, Hunter College of the City University of New York, 695 Park Avenue, New York, New York 10021

Received December 7, 1992

The steady-state and transient dynamics of phase locking in a two-element Nd:YAG laser array have been studied. By creating two evanescent-coupled lasers in a Nd:YAG étalon using diode end pumping, the coupling strength between the laser elements in the array can be continuously varied by adjusting the positions of the pumping beams. This allows the observation of the phase-locking process over a wide range of coupling strength. We have found that the development of the phase-locked state is as fast as the onset of lasing without an evolutionary process. The instantaneous locking is also independent of the coupling strength once the coupling is strong enough to ensure phase locking. These phenomena disagree with the predictions based on the time-dependent coupled-mode theory of laser-array dynamics. Our experimental study and theoretical analysis have led to the conclusion that all predictions of optical instability in laser arrays need to be reexamined.

The dynamics of phase locking in evanescent coupled laser arrays has been a subject of considerable interest in recent years. Sustained pulsation and irregular spiking phenomena in the picosecond time scale have been observed in the semiconductor laser arrays.<sup>1</sup> These phenomena have been attributed to the nonlinear interaction between oscillators.<sup>2,3</sup> While the dynamics of coupled lasers has been extensively modeled in recent literature,<sup>2-7</sup> there has been no systematic experimental confirmation of the theoretical predictions. Most of the laser arrays used in the previous experimental studies contained a large number of elements. The complexity of the system of a 10-element array (often containing 10 sets of differential equations of field amplitude, phase, and population inversion<sup>1</sup>) makes it difficult to relate the observed phenomena to the device parameters. Furthermore, there also exists discrepancy between the observed and predicted dynamical behavior. For example, the development of phase locking in a semiconductor laser array is found to take place within 100 ps.<sup>1</sup> However, the numerical modeling based on the rate equations for the electric fields with a coupling term predicted a time constant of the order of 10 ns.<sup>2</sup>

In this Letter we report an experimental study of phase locking in a two-element evanescent-wave-coupled Nd:YAG laser array. The two-element array has the fewest numbers of dynamic variables. Compared with semiconductor lasers, Nd:YAG is a simpler system because there is no amplitude-phase coupling and other complications such as gain guiding and carrier diffusion.<sup>7</sup> We believe that this Nd:YAG laser array provides the most transparent system for establishing the essence of the phase-locking processes. With diode pumping, the separation between the elements can be continuously varied by adjusting the positions of the pumping beams. This enables us to investigate the dynamics of the array for a wide range of coupling strength to provide a test of the predictions of nonlinear dynamics based on the

coupled-mode analysis. Recently, a similar photo-pumping technique has been used for studying the coherence and noise characteristics in a two-element Nd:YAG laser array.<sup>8</sup>

The experimental setup and the far-field profile of the laser array are shown in Fig. 1. Two 808-nm AlGaAs/GaAs diode lasers are used to end pump a Nd:YAG étalon to create two lasing filaments, each operating in the fundamental transverse mode. The diameter of the pumping beams is 50  $\mu\text{m}$ . The threshold pumping power is 80 mW. The two end surfaces of the YAG étalon are polished flat and parallel to within 1 arcsec and are coated for 100% and 95% reflectivity at 1064 nm. The residual wedge of the étalon results in a detuning as high as a few megahertz between the two elements owing to the small cavity length difference. The frequency detuning can be eliminated by rotating the étalon about the axis of propagation.

The transverse mode of the individual element is mainly determined by the thermally induced refractive-index waveguide.<sup>9</sup> In Nd:YAG, the refractive-index increase,  $\Delta n_T$ , with respect to temperature is  $7 \times 10^{-6}/\text{K}$ .<sup>10</sup> The thermally induced refractive-index change can be measured by the shift of the beat frequency of two unlocked laser elements as the pump power of one of the elements

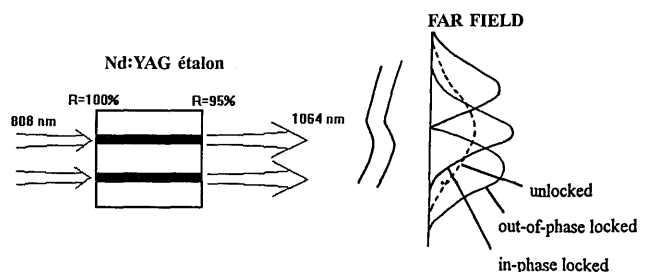


Fig. 1. Configuration of the diode-end-pumped two-element laser array in a Nd:YAG étalon. On the right is the far-field profile.

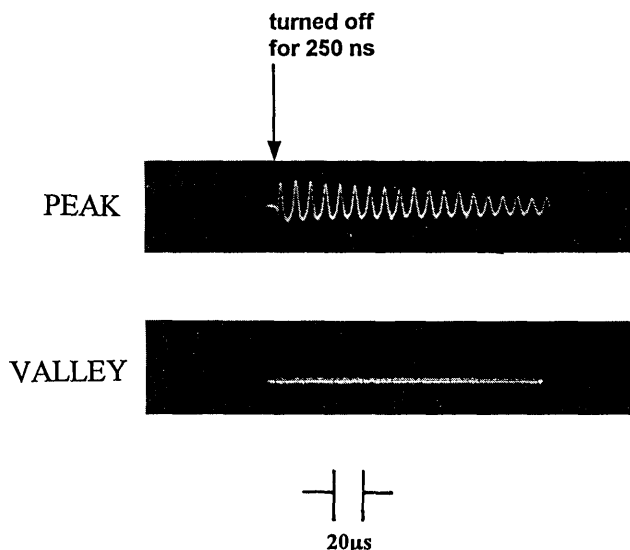


Fig. 2. Time series of intensities measured at the peak (upper trace) and valley (lower trace) of the far-field distribution. The 250-ns turned-off period is not resolved in this time scale.

is varied. In our experiment, the refractive-index step is measured to be  $2 \times 10^{-6}$ , corresponding to a temperature rise of 0.3 K. The imaginary part of the refractive index, estimated from the mirror loss of the cavity, is  $4 \times 10^{-7}$ .

When the two elements are separated by a large distance, the far-field pattern has a Gaussian-like pattern that is the incoherent addition of the patterns of the individual elements. Phase locking is observed when the separation is less than  $1000 \mu\text{m}$ , corresponding to a coupling strength<sup>11</sup> of  $5 \times 10^{-4}$ . At this point, the far-field intensity distribution exhibits a two-lobed pattern with a dark fringe at the center, as expected of the interference pattern of two coherent sources with a phase difference of  $\pi$ .

To study the turn-on dynamics of the laser arrays, the cw laser arrays are momentarily turned off for a 250-ns period, and the recovery process from below the threshold to the steady-state intensity is recorded. Figure 2 shows the simultaneous time series of the intensities measured with two detectors placed at the peak and the valley of the far-field intensity distribution. The intensity undergoes a simple relaxation oscillation whose damping time constant is comparable with that of the relaxation oscillation of the individual element. Most notably, the intensity at the center of the far-field pattern is zero as soon as the lasing begins and remains the same throughout the process. This suggests that phase locking is developed as fast as the occurrence of the first peak of the relaxation oscillation, and the development of phase locking does not undergo an evolutionary process. Furthermore, once the coupling is strong enough to ensure phase locking, the fast locking is independent of the coupling strength. We have also found that any perturbation in the pumping power of one of the elements is instantly transmitted to the other without a time delay.

We have first attempted to model the array dynamics by treating the effect of coupling by a coupling

term between electrical fields of two identical lasers as was done in previous treatments.<sup>2-6</sup> The equations are

$$\frac{dE_1}{dt} = \frac{g_1'}{2}(N_1 - N_{\text{th}})E_1 + \frac{\kappa c}{n}[E_2 \sin(\Delta\varphi)], \quad (1)$$

$$\frac{dE_2}{dt} = \frac{g_2'}{2}(N_2 - N_{\text{th}})E_2 + \frac{\kappa c}{n}[E_1 \sin(\Delta\varphi)], \quad (2)$$

$$\frac{d(\Delta\varphi)}{dt} = \frac{\kappa c}{n} \left( \frac{E_2}{E_1} - \frac{E_1}{E_2} \right) \cos(\Delta\varphi) + \Delta\omega, \quad (3)$$

$$\frac{dN_1}{dt} = P - \frac{N_1}{\tau_s} - \left[ \frac{1}{\tau_p} + g_1'(N_1 - N_{\text{th}}) \right] E_1^2, \quad (4)$$

$$\frac{dN_2}{dt} = P - \frac{N_2}{\tau_s} - \left[ \frac{1}{\tau_p} + g_2'(N_2 - N_{\text{th}}) \right] E_2^2, \quad (5)$$

where  $N_i$  is the population inversion,  $E_i$  is the field amplitude of the individual lasers, and  $\Delta\varphi$  is the phase difference of the two elements. The other parameters are the differential gain  $g'$ , the coupling coefficient  $\kappa = \eta n/c\tau_p$ , the threshold population inversion  $N_{\text{th}}$ , the frequency detuning  $\Delta\omega$ , the pump rate  $P$ , the photon lifetime  $\tau_p$ , and the lifetime of the excited state  $\tau_s$ . The calculated intensities at the valley and peak of the two-lobed far-field pattern, corresponding to  $E_1^2 + E_2^2 + 2E_1E_2 \cos(\Delta\varphi)$  and  $E_1^2 + E_2^2 - 2E_1E_2 \cos(\Delta\varphi)$ , are shown in Figs. 3(a) and 3(b). The transition process is characterized by beam

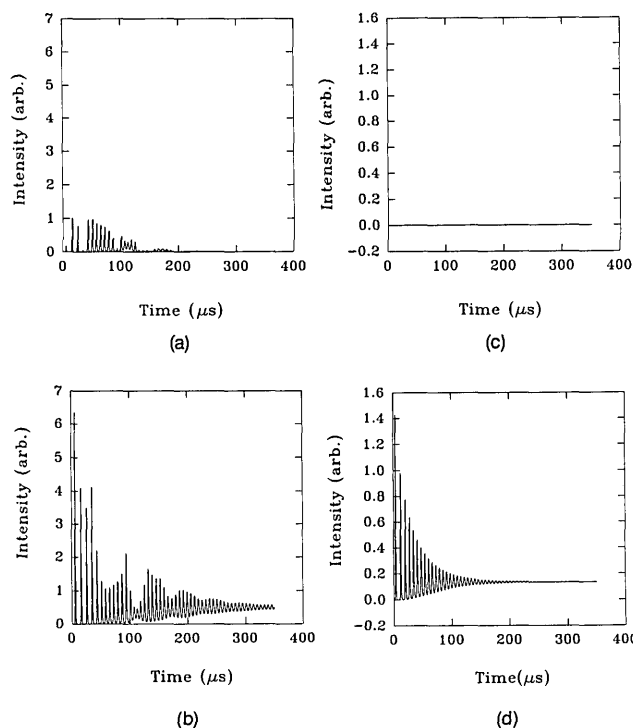


Fig. 3. Time series of intensities at (a) the valley and (b) the peak of the far-field intensities calculated using  $E_1$  and  $E_2$  as the basis; (c) and (d) are the corresponding intensities calculated using  $\psi_{\text{II}}$  and  $\psi_{\text{II}}$  as the basis. The parameters are  $\tau_p = 5 \text{ ns}$ ,  $\tau_s = 200 \mu\text{s}$ ,  $\eta = 10^{-3}$ , and  $g_1' = g_2' = 10^{-17} \text{ m}^3/\text{s}$  for (a) and (b); the mode gain difference is 1% for (c) and (d).

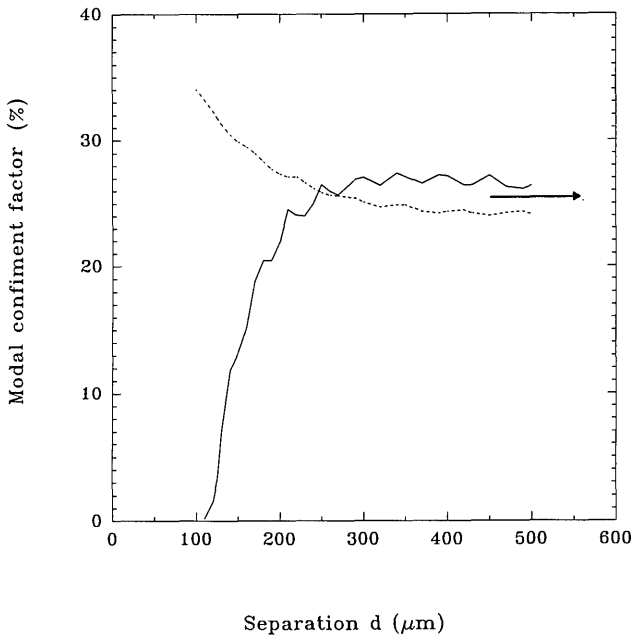


Fig. 4. Calculated modal confinement factors for the two eigenmodes of the composite waveguide as the function of the separation between the waveguides. The dotted curve denotes the symmetric mode, the solid curve denotes the antisymmetric mode, and the arrow denotes the mode of the individual waveguide.

scanning in the far field caused by the oscillation of the relative phase. Because of this oscillation in phase, the envelopes of the relaxation oscillation in Figs. 3(a) and 3(b) are anticorrelated. The time constant for the establishment of the phase-locked state is of the order of 300  $\mu$ s. However, as shown in Fig. 3, the modeling cannot explain the observed instant locking. While the inclusion of the imaginary part of the coupling strength tends to shorten the time of phase locking, the instant locking cannot be explained with any complex coupling strength of a realistic magnitude. Furthermore, the coupled-oscillator theory predicts that the perturbation to one of the elements could be felt by the other after an energy-transfer time.<sup>5</sup> This again disagrees with the observation of instant transmission.

These disagreements have prompted us to reexamine the coupled-mode model. The previously ascribed view on laser arrays is treating each laser with individual gain as an individual oscillator and then coupling them together nonlinearly to produce the phase-locked output. The implicit assumption is that the individual laser can oscillate first. Instead, our numerical calculation for the waveguide structure indicates that this basic assumption is violated. As shown in Fig. 4, the numerically calculated confinement factors for the eigenmodes of the composite waveguide are always higher than that of the individual waveguide. Thus the analysis using the eigenmodes of the individual waveguides,  $E_1$  and  $E_2$ , as the bases is not applicable because these modes cannot oscillate owing to the less favorable gains.

The appropriate choice of bases would be the in- and out-of-phase modes,  $\psi_{\parallel}$  and  $\psi_{\perp}$ , of the composite waveguide. These two orthogonal modes can be described by standard two-mode rate equations, and the state of operation is determined by the competition between two modes. The calculated intensities at the minimum and maximum intensities of the far field, corresponding to  $\psi_{\parallel}^2$  and  $\psi_{\perp}^2$ , are shown in Figs. 3(c) and 3(d). With a modal gain difference of 1%, the out-of-phase mode is established from the start, and the system undergoes a damped relaxation oscillation, as observed experimentally.

In a generic sense, we can put the above in the following light. In a laser system, the spontaneous emission photons that experience the largest modal gain (or the least threshold) can initiate the lasing. In our case, the mode of the lowest threshold is the eigenmode of the composite waveguide, not that of the individual waveguide. Since the phase-locked mode is initiated by spontaneous emission, the phase locking can be developed as fast as the first peak of the relaxation oscillation as observed experimentally.

Finally, we provide an alternative explanation for the pulsing phenomenon observed in semiconductor laser arrays,<sup>1</sup> which has been widely cited as the evidence of instabilities in laser arrays.<sup>2-7</sup> The 10-element semiconductor laser arrays are known to operate in a number of supermodes, separated by 0.03 nm.<sup>1,12</sup> The complex pulsation in the 100-ps time scale is expected owing to the beating among the supermodes.

## References

1. R. A. Elliot, R. K. Defreez, T. L. Paoli, R. D. Burnham, and W. Streifer, *IEEE J. Quantum Electron.* **QE-21**, 598 (1985).
2. S. S. Wang and H. G. Winful, *Appl. Phys. Lett.* **53**, 1894 (1988).
3. S. S. Wang and H. G. Winful, *Appl. Phys. Lett.* **52**, 1774 (1988).
4. R. K. Jakobsen, R. A. Indik, J. V. Moloney, A. C. Newell, H. G. Winful, and L. Raman, *J. Opt. Soc. Am. B* **8**, 1674 (1991).
5. K. Otsuka, *Phys. Rev. Lett.* **65**, 329 (1990).
6. H. G. Winful and L. Rahman, *Phys. Rev. Lett.* **65**, 1575 (1990).
7. L. Rahman and H. G. Winful, in *Digest of Topical Meeting on Nonlinear Dynamics in Optical Systems* (Optical Society of America, Washington, D.C., 1992), paper ThB3.
8. L. Fabiny, P. Colet, and R. Roy, in *Digest of Topical Meeting on Nonlinear Dynamics in Optical Systems* (Optical Society of America, Washington, D.C., 1992), paper ThB2.
9. M. Oka, H. Masuda, Y. Kaneda, and S. Kubota, *IEEE J. Quantum Electron.* **28**, 1142 (1992).
10. W. Koechner, *Solid State Laser Engineering* (Springer-Verlag, Berlin, 1992), p. 51.
11. A. Yariv, *Quantum Electronics*, 3rd ed. (Wiley, New York, 1989), Chap. 22.
12. T. L. Paoli, W. Streifer, and R. D. Burnham, *Appl. Phys. Lett.* **45**, 217 (1984).